

Additional file 1

Effect of vacancies and edges in promoting water chemisorption on titanium-based MXenes

Edoardo Marquis, Francesca Benini, Babak Anasori, Andreas Rosenkranz, and Maria Clelia Righi*

E. Marquis, F. Benini, Prof. M. C. Righi

Department of Physics and Astronomy, Alma Mater Studiorum – University of Bologna, Viale Berti Pichat 6/2, 40127, Bologna, Italy

*E-mail: clelia.righi@unibo.it

Prof. B. Anasori

School of Materials Engineering, Purdue University, West Lafayette, Indiana 47907, USA

Prof. A. Rosenkranz

Department of Chemical Engineering, Biotechnology and Materials, University of Chile, Avenida Beaucheff 851, 8370456, Santiago de Chile, Chile

Computational Details

MXenes 4x4 orthorhombic cells are modelled starting from hexagonal unit cells, which are exemplarily shown in **Figure S1a** (top view of Ti_2CO_2). To optimize the in-plane lattice parameter, 'a', for the hexagonal cells, we carried out multiple calculations of structural optimization for different values of 'a'. During these relaxations, the vertical lattice parameter, 'c', was kept fixed to ensure a vacuum region of about 15 Å along z. An ordinary least squares regression was used to fit the energies as a function of 'a' with a parabolic function, thus identifying the minimum. We repeated the procedure for different wave-function cutoffs (the charge density cutoff was always set as eight times the wave-function cutoff), as reported in **Figure S1b**. The convergence test for K-points grid is also displayed in **Figure S1c** for the hexagonal unit cell. An equivalent grid was used for 4x4 orthorhombic cells, corresponding to a 3x4x1 grid.

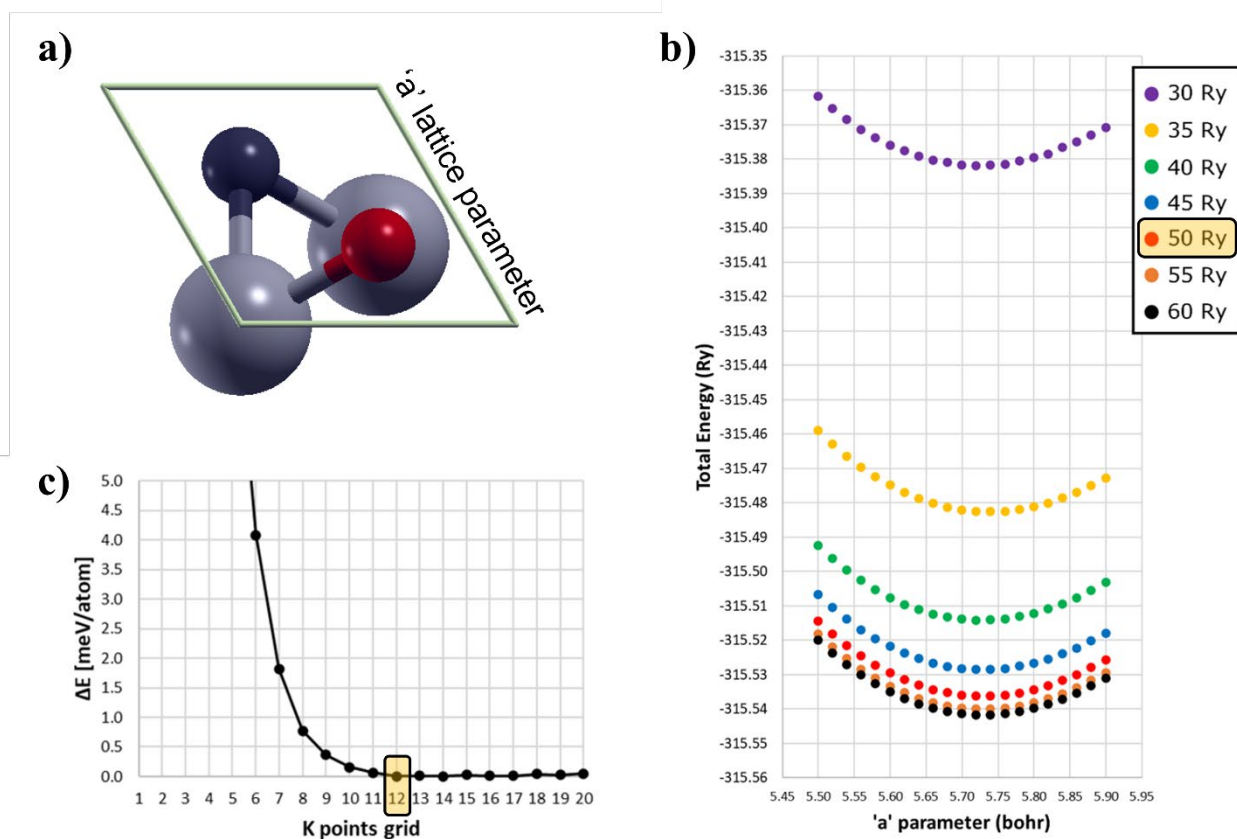


Figure S1. a) Top-view of the hexagonal unit cell for Ti_2CO_2 (Ti, C and O atoms are shown in grey, black and red colour, respectively). (b) Convergence test for the electronic wave-function cut-offs: the optimization of the 'a' lattice parameter is repeated for different cut-off values. We have chosen a plane-wave (charge density) cut-off of 50Ry (400Ry). (c) Convergence test for the $N_xN_xN_z$ Monkhorst-Pack grid. The convergence for the hexagonal cell is reached with a grid of 12x12x1.

Supercells

MXene' orthorhombic supercells were built based on their hexagonal unit cell. In **Figure S2**, we depict an example of the 4x4 orthorhombic supercells employed in our work, corresponding to the cases of defect-free Ti_2CF_2 and $\text{Ti}_4\text{C}_3\text{F}_2$. Surfaces with defects have been modelled with the same 4x4 supercell.

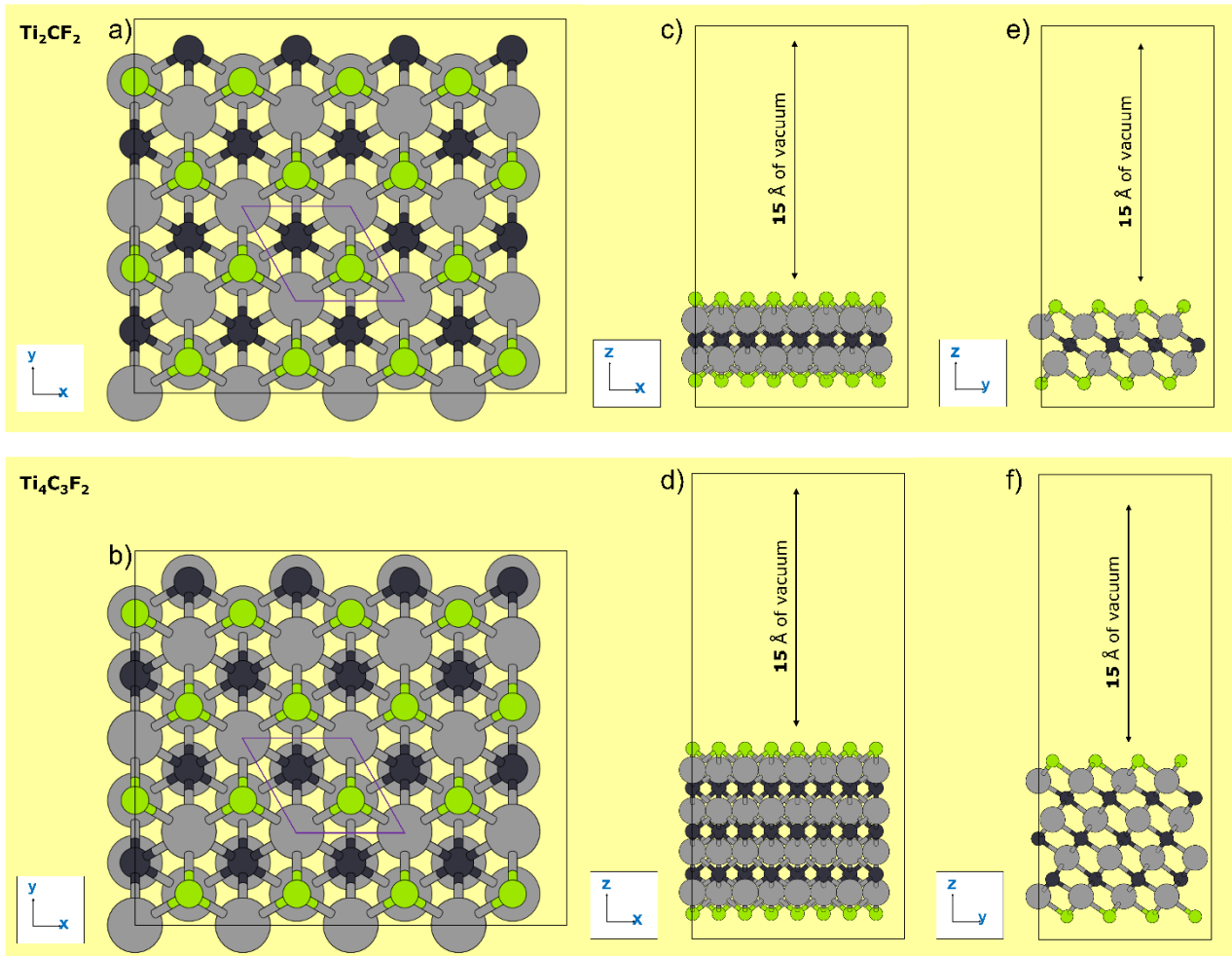


Figure S2. (a-b) Top views and (b-f) side views for the 4x4 orthorhombic supercells used for Ti_2CF_2 and $\text{Ti}_4\text{C}_3\text{F}_2$. The original hexagonal unit cell is indicated in purple in the top view (left).

MXene nanoribbons were built starting from the 4x4 orthorhombic supercells by doubling the length of the b lattice parameter (along the y axis). The supercell employed is depicted in **Figure S3** for the case of $\text{Ti}_8\text{N}_3(\text{OH})_8$.

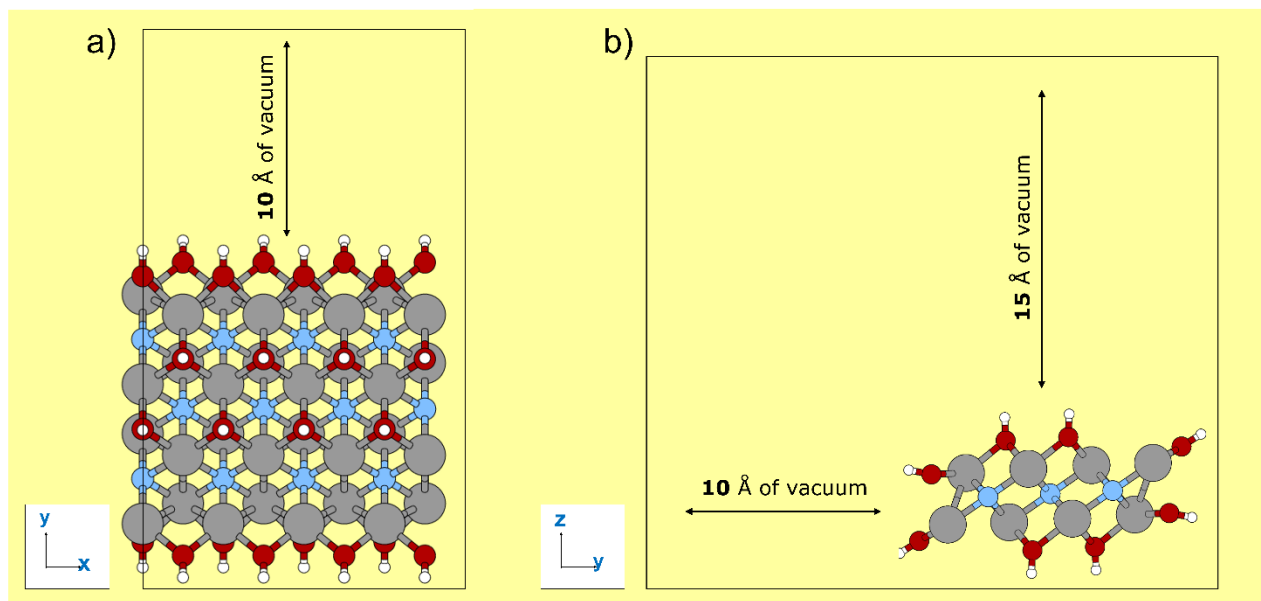


Figure S3. (a) Top and (b) side view of 1D $\text{Ti}_8\text{N}_3(\text{OH})_8$. The ribbon grows along the x direction. Vacuum is required along y and z axes to avoid the lateral interactions between replicas.

Sampling of water configurations

To explore different adsorption minima, several initial configurations concerning the orientation of water were considered for each substrate, as exemplarily shown in **Figure S4** for V_{Ti} on Ti_2CF_2 .

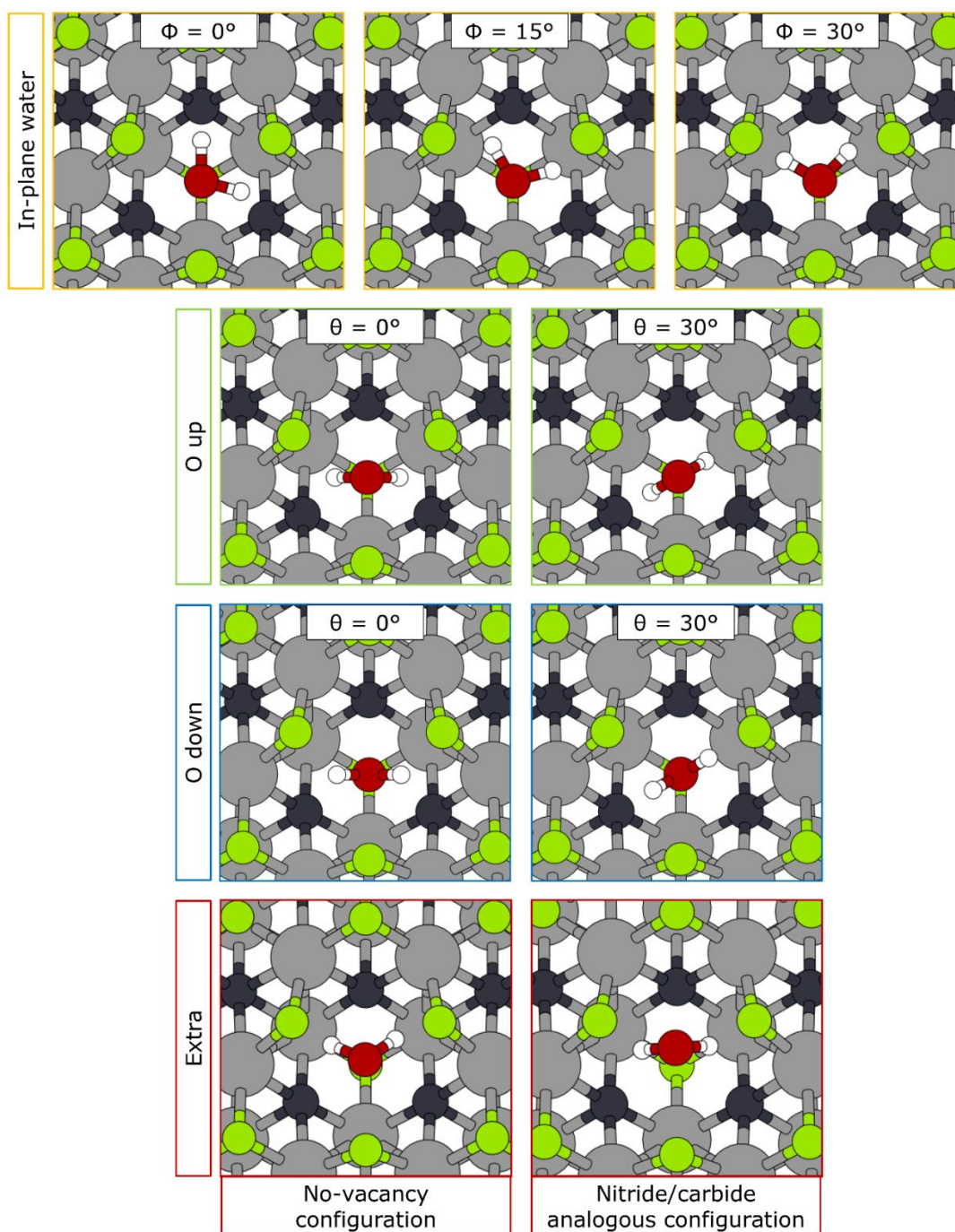


Figure S4. Input geometries of H_2O explored to find the absolute minimum. Ti_2CF_2 surfaces with a missing Ti atom are exemplarily considered. However, it is important to point out that the same procedure has been adopted for all cases. We tried different water orientations such as in-plane, oxygen-up and oxygen-down. Rotations of the water molecule have also been tested, considering the internal symmetries of the surface ($0^\circ < \theta < 30^\circ$). In addition, two extra H_2O configurations have been tried: the one obtained from the H_2O optimization on the full-terminated surface, and the one from the optimization of H_2O on the analogous nitride (or carbide).

Configurations of water physically adsorbed on surface with $V_{C/N}$ and V_{Ti}

In **Figure S5**, we provide the relaxed configurations for H_2O interacting with defective Ti_2CO_2 and $Ti_2C(OH)_2$, which have not been included in the main manuscript. Ti_2CO_2 is also representative for the nitride and F-terminated analogs. In contrast, $Ti_2C(OH)_2$ is representative for $Ti_2N(OH)_2$.

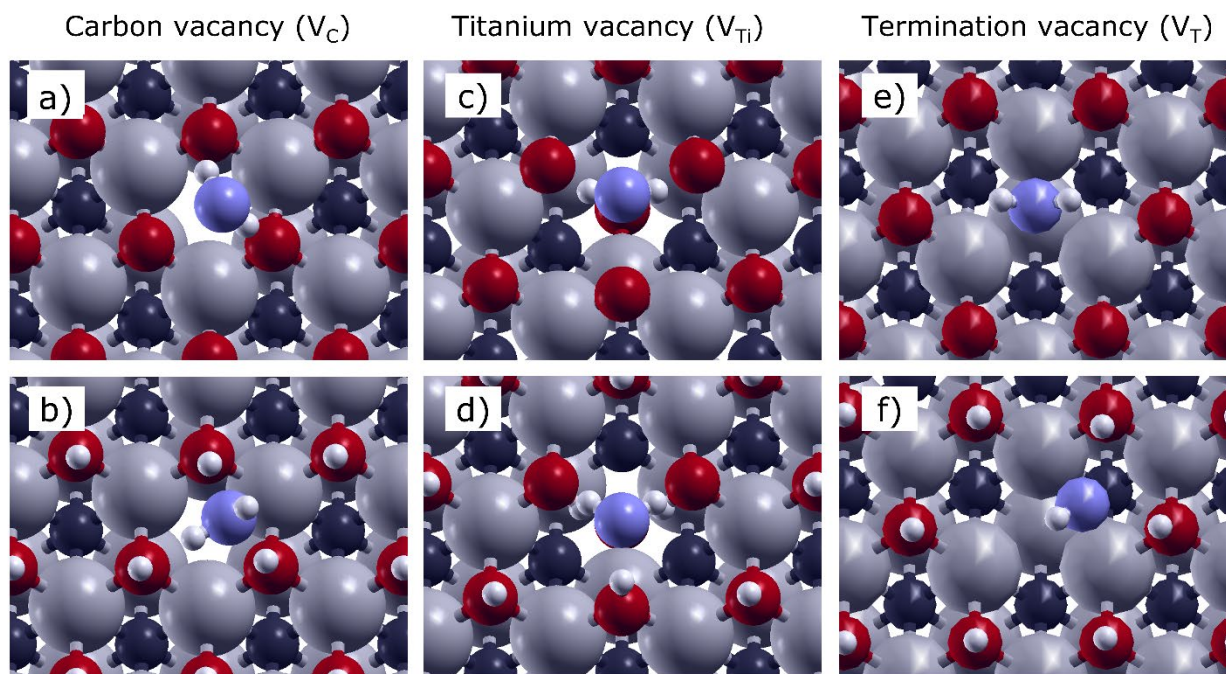


Figure S5. Top view of the relaxed configuration of H_2O on surfaces with a single atom vacancy: (a-b) carbon vacancy, (c-d) titanium vacancy, (e-f) termination vacancy. (a, c and e) Ti_2CO_2 and (b, d and f) $Ti_2C(OH)_2$ are taken as examples. The oxygen atom of the water molecule is depicted in purple color to differentiate it from the other O atoms on the surface (in red). The interaction between water and defective surface occurs via H-bonds, apart from the case of Ti_2CO_2 with a termination missing (e), as discussed in the main manuscript.

Nanoribbons and H₂O-edge configurations

In **Figure S6**, we provide the relaxed, cross-sectional configurations of the nanoribbons discussed in the main manuscript, as well as the top view of H₂O interacting with the edges.

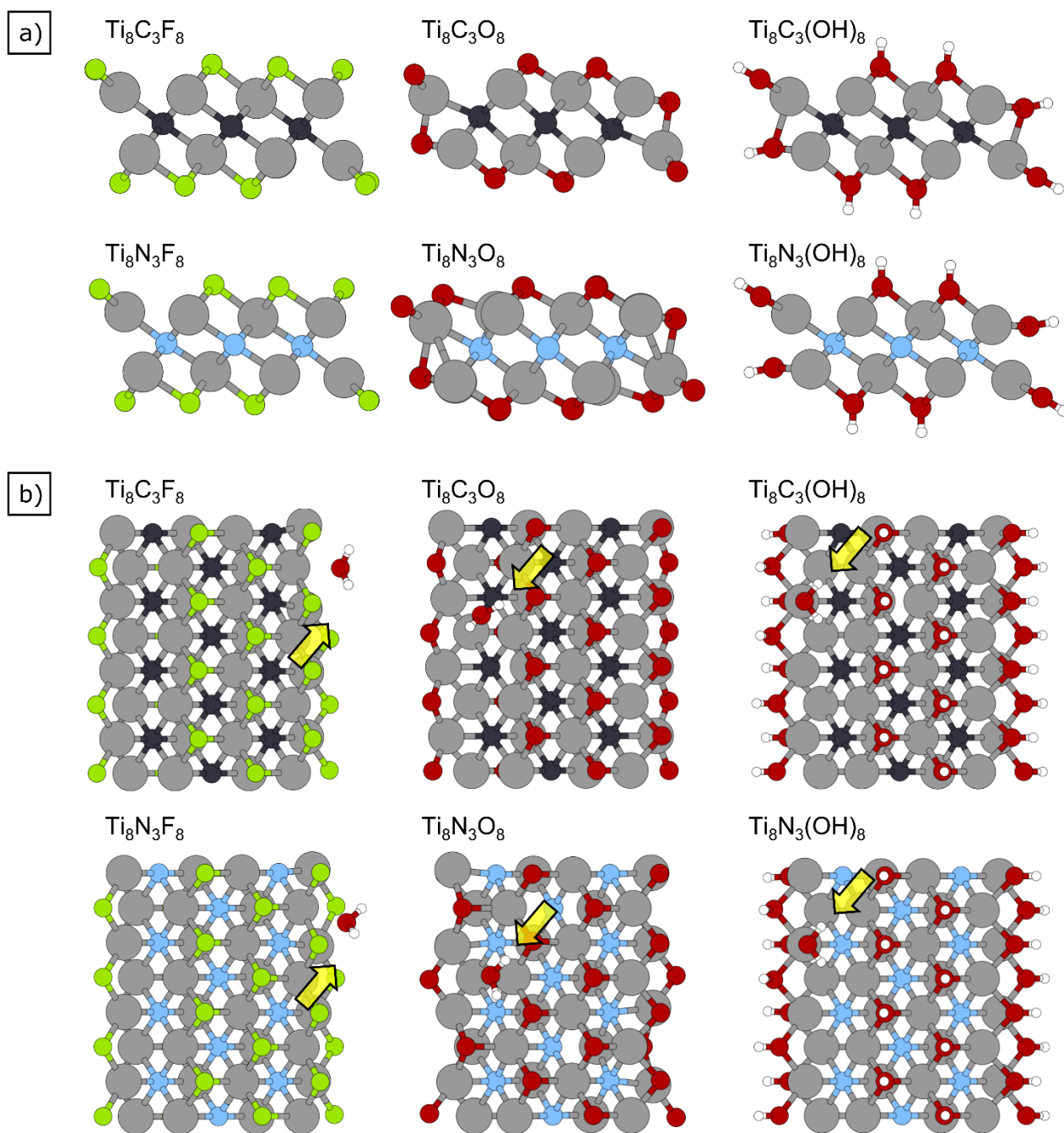


Figure S6. (a) Cross-sectional view of the $\text{Ti}_8\text{X}_3\text{T}_8$ nanoribbons and (b) top view of the chemisorbed water on nanoribbons, with $\text{X} = \text{C}$ or N , and $\text{T} = \text{F}$, O or OH . The transparent arrow in yellow highlights the presence of the water molecule.

Configurations of water chemisorbed on surface with cluster of vacancies $2V_{Ti} + qV_T$ with $q = 1, 2, 3$

In **Figure S7**, we present the relaxed configurations of H_2O interacting with $2V_{Ti} + qV_T$ ($q = 1, 2, 3$) defect clusters on Ti_2CF_2 and $Ti_2C(OH)_2$. The chemisorption of water on $2V_{Ti} + qV_T$ clusters ($q = 1, 2, 3$) is regulated by almost the same mechanisms discussed in the main manuscript for $1V_{Ti} + qV_T$ clusters. The most relevant difference is the number of Ti atoms interacting with the oxygen atom of H_2O (i.e., stabilized by the oxygen of H_2O). For instance, the presence of a double V_{Ti} in the cluster $2V_{Ti} + 1V_T$ (Figure S6 a-b) leaves only one titanium atom with dangling bonds (indicated with a tiny yellow arrow in Figure S6). Apart from these structural differences, energy gains related to the chemisorption of water are always greater than 1eV.

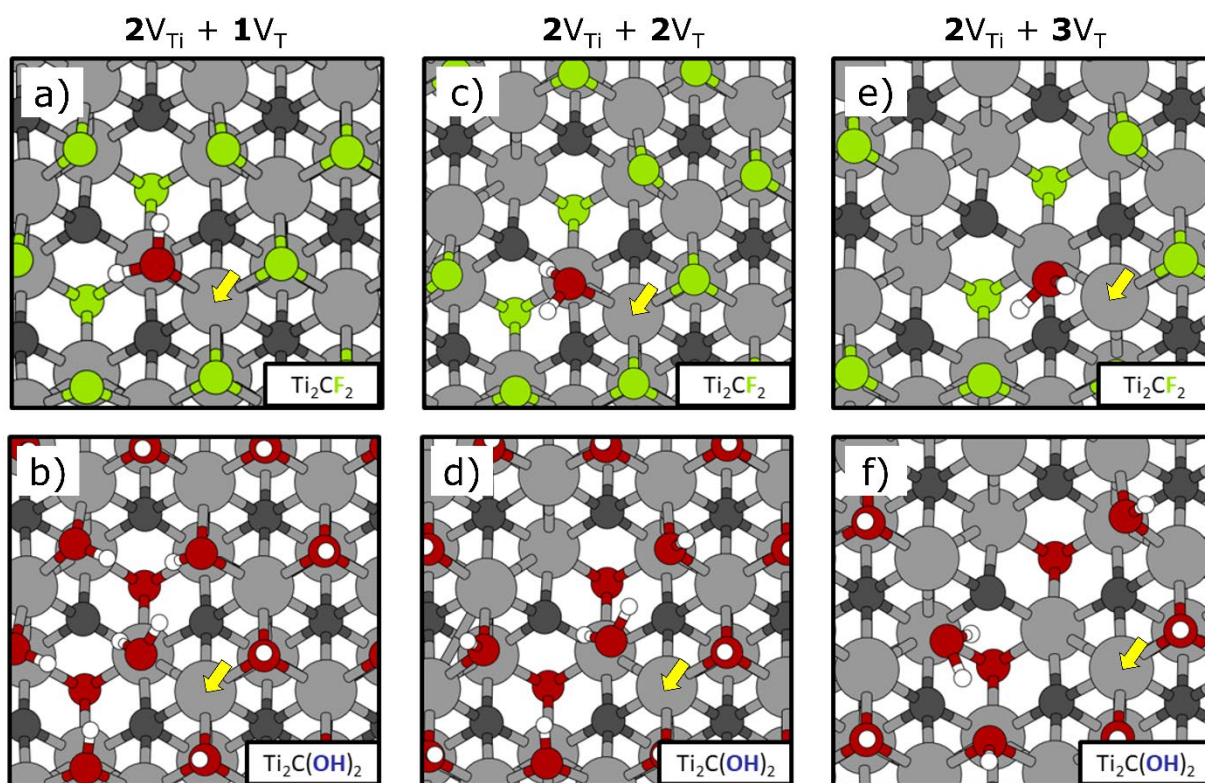


Figure S7. Top view for the optimized configurations of H_2O chemisorbed on (a, c and e) Ti_2CF_2 and (b, d and f) $Ti_2C(OH)_2$ with $2V_{Ti} + qV_T$ (with $q=1, 2, 3$) vacancy clusters. The oxygen of the water molecule interacts with the remaining undercoordinated Ti atom highlighted by a tiny yellow arrow, apart from panel f, for which it stabilizes two Ti atoms instead of one.

Energy gain VS H₂O---Ti distances

For $1V_{Ti}+qV_T$ (with $m = 1,2,3$) and $2V_{Ti}+1V_T$ clusters, the water molecule interacts similarly with all the substrates, regardless of the termination type. The oxygen atom of H₂O saturates a V_T , interacting with one/two remaining Ti atom(s), while one hydrogen atom of H₂O is pointed towards the hole left by V_{Ti} . $Ti_2C(OH)_2$ and $Ti_2N(OH)_2$ are exceptions for the cluster of defects $1V_{Ti}+1V_T$, as mentioned in the main manuscript in section 3.5. We found a correlation between the energy gain related to water chemisorption and the average distance between the oxygen of H₂O and the two Ti atoms (**Figure S8**).

Moreover, the average bond distance between H₂O and the involved Ti atom is found to be strongly reduced for chemisorption on $2V_{Ti}+1V_T$ clusters, comparable to the typical bond distance between Ti and T in a defect-free layer. The lilac squares on the left in Figure S7a, which relate to $2V_{Ti}+1V_T$ clusters, are shifted towards shorter H₂O---Ti distances.

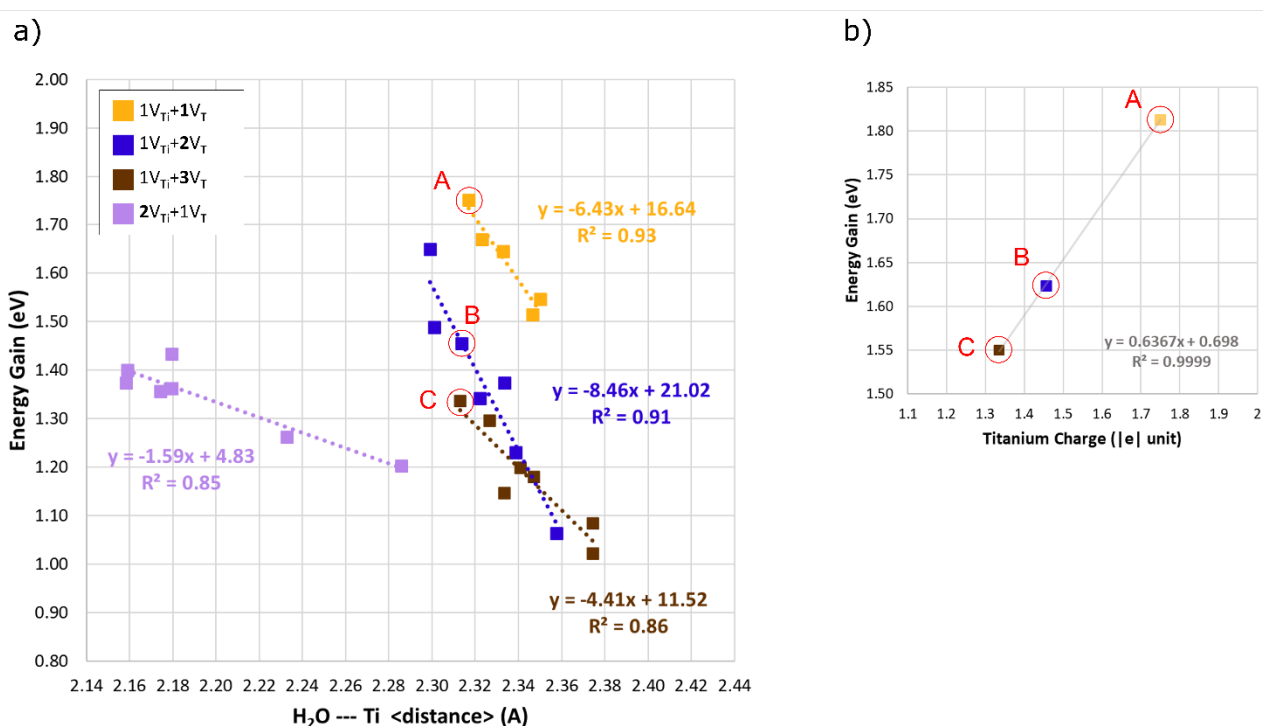


Figure S8. a) Energy gain versus average distance between the oxygen of H₂O and two Ti atoms. The linear regressions highlight the correlations. Three points showing the same “H₂O --- Ti <distance>”, while owing to different clusters of defects ($1V_{Ti}+1V_T$, $1V_{Ti}+2V_T$ and $1V_{Ti}+3V_T$), have been selected. For these cases, we calculated the partial atomic charges of the Ti atoms involved in the interaction with water, and we correlated with the corresponding energy gains (inset b). The higher the charge of Ti, the greater is the energy gain.

Effect of water coverage for Ti_2CF_2 , $\text{Ti}_4\text{C}_3\text{F}_2$, Ti_2NF_2 , and $\text{Ti}_2\text{N}(\text{OH})_2$

The dependance of the energy gain on the water coverage from 6% to 100% is reported in **Figure S9** for all the considered defect-free surfaces. Ti_2NO_2 is excluded as its reactivity towards water leads to structural degradation.

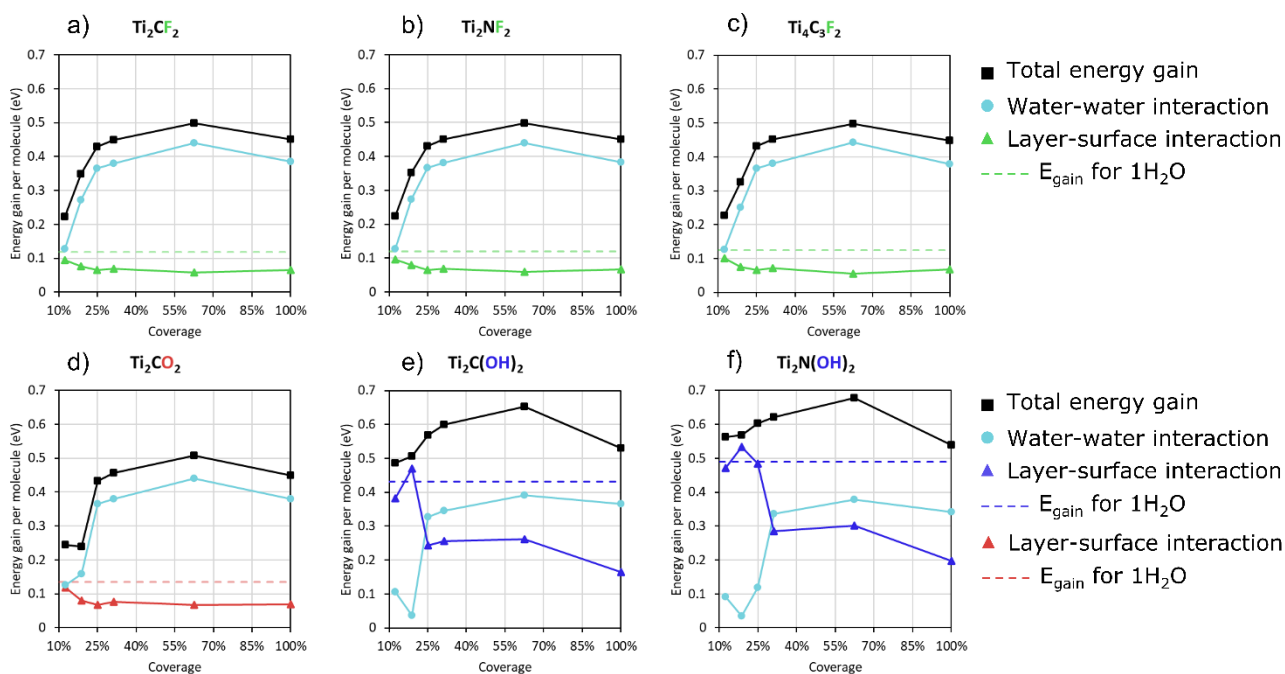


Figure S9. Energy gain per molecule as a function of the water coverage for (a) Ti_2CF_2 , (b) Ti_2NF_2 , (c) $\text{Ti}_4\text{C}_3\text{F}_2$, (d) Ti_2CO_2 , (e) $\text{Ti}_2\text{C}(\text{OH})_2$ and (f) $\text{Ti}_2\text{N}(\text{OH})_2$. Both contributions (water-water and layer-surface interaction) to the total energy (black line) are separately shown. The interaction between the water molecules is highlighted in light blue. The interaction between the water layer and the substrate is colored depending on the type of termination. The dashed line indicates the interaction value for a single water molecule, corresponding to a coverage of 6%. O- and F-terminated MXenes behave almost identically, while OH-terminated carbide and nitride show a similar trend as well.

Charge analysis

The correlation between the energy gain related to H₂O chemisorption and the residual partial atomic charge on titanium have been discussed in the main manuscript for V_T substrates. In **Figure S10**, we collect the calculated Bader charges on V_T substrates.

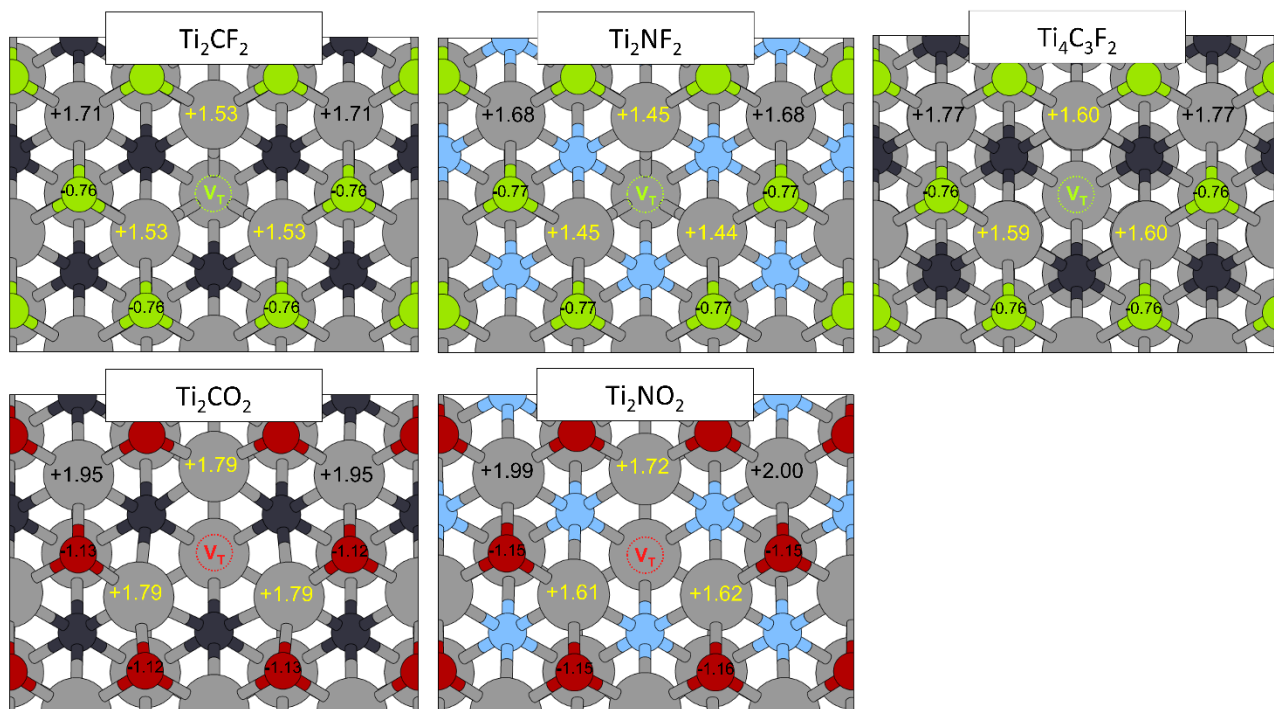


Figure S10. Calculated Bader charges are indicated on the -O/-F terminations and Ti atoms surrounding the vacancy of termination (V_T). The three titanium atoms close to the vacancy show a lower positive charge than the defect-free case.

Optimized structures of MXene substrates

A selection of relaxed MXene substrates employed in our work is reported in **Figure S11**, **Figure S12** and **Figure S13**.

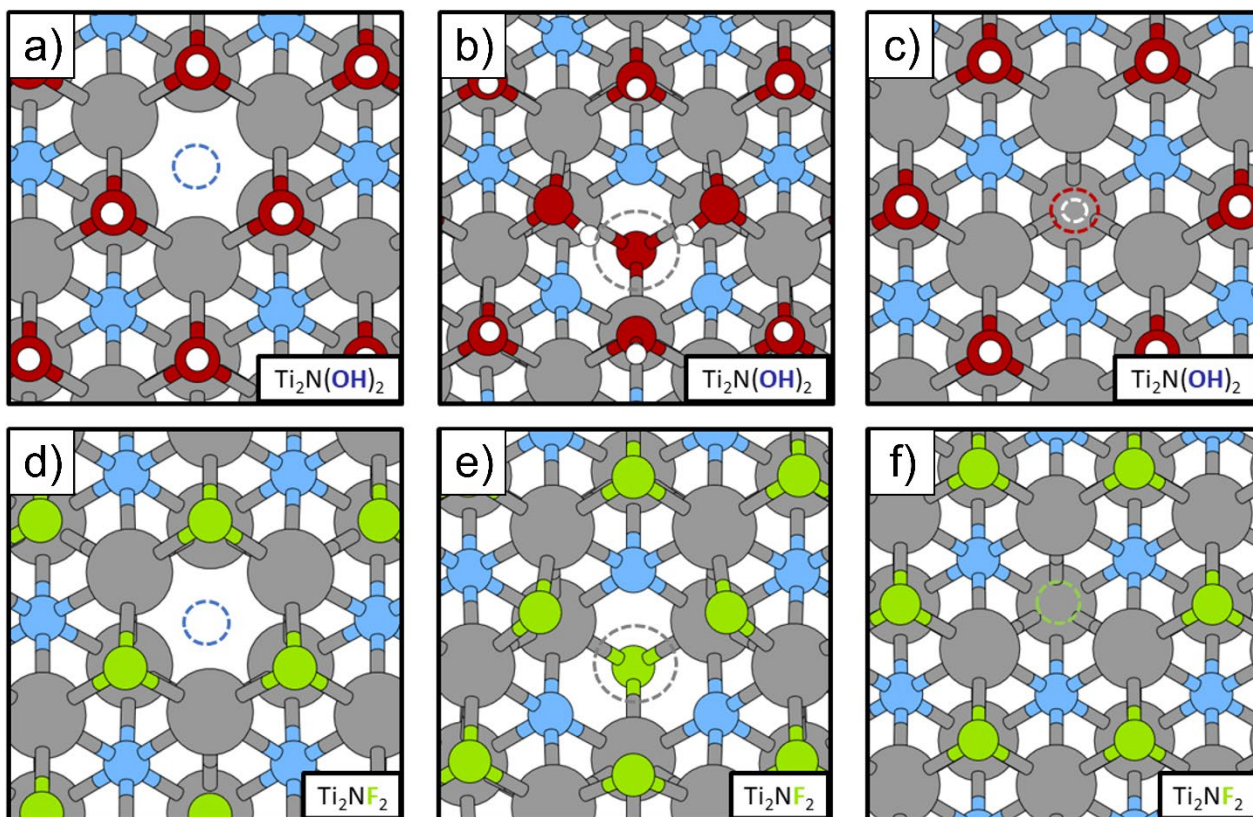


Figure S11. Top view of relaxed surfaces with a single vacancy for (a-c) $\text{Ti}_2\text{N}(\text{OH})_2$ and (d-f) Ti_2NF_2 . (a and d) Single vacancy of one N atom (V_N). (b and e) Single vacancy of one Ti atom (V_{Ti}). (c and f) Single vacancy of a termination (V_T). Missing atoms are indicated with dashed circles. A surface reconstruction is observed only for V_{Ti} (b and e), consisting of a displacement of the surrounding terminating groups that move closer to the two remaining Ti atoms to interact more strongly. For the case of a V_{Ti} vacancy on the OH-terminated surface (b), hydroxyl groups can rotate to point their hydrogen atom towards the Ti vacancy.

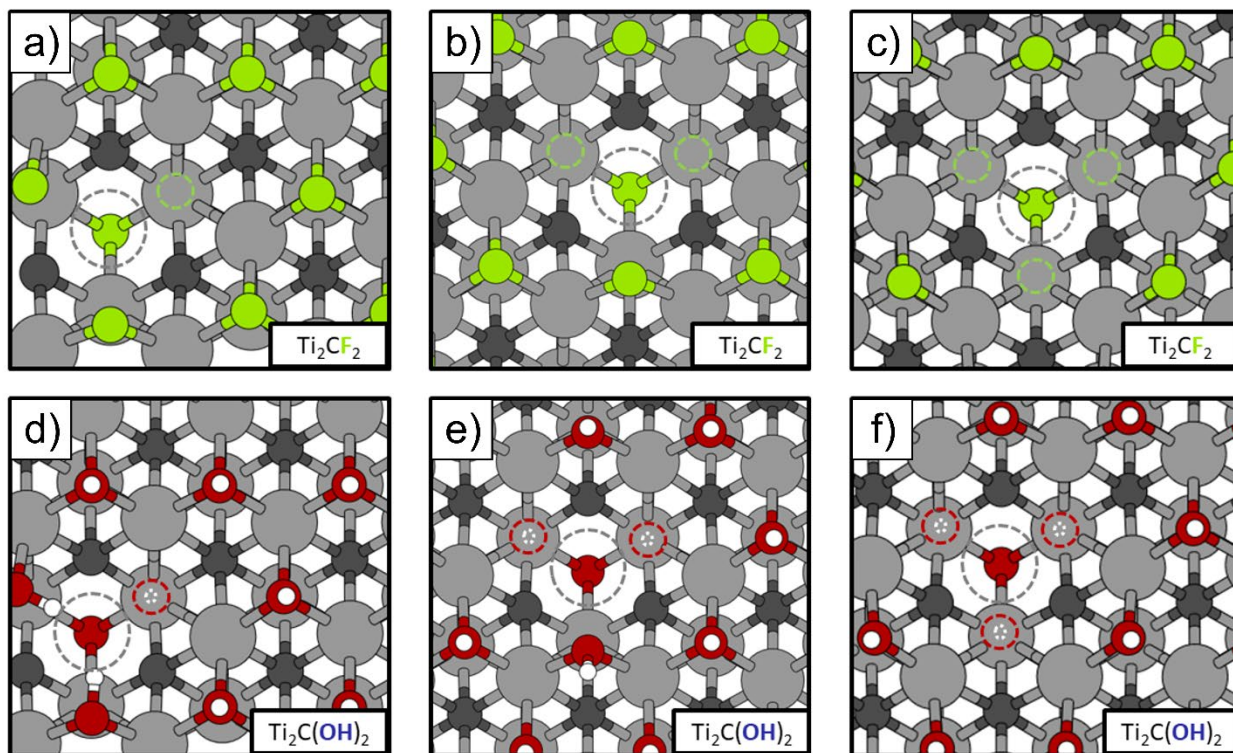


Figure S12. Relaxed surfaces with $1V_{\text{Ti}} + qV_{\text{T}}$ (with $m=1,2,3$) clusters of vacancies for (a-c) Ti_2CF_2 and (d-f) $\text{Ti}_2\text{C}(\text{OH})_2$. (a and d) $1V_{\text{Ti}} + 1V_{\text{T}}$ cluster; (b and e) $1V_{\text{Ti}} + 2V_{\text{T}}$ cluster; (c and f) $1V_{\text{Ti}} + 3V_{\text{T}}$ cluster. Missing atoms are indicated with dashed circles. Due to the hole caused by the V_{Ti} , the surrounding terminating groups move closer to the remaining Ti atoms to interact more strongly. For OH-terminated surfaces (d-f), the remaining hydroxyls can rotate to point their hydrogen atom towards the Ti vacancy, providing a stabilization to the defect.

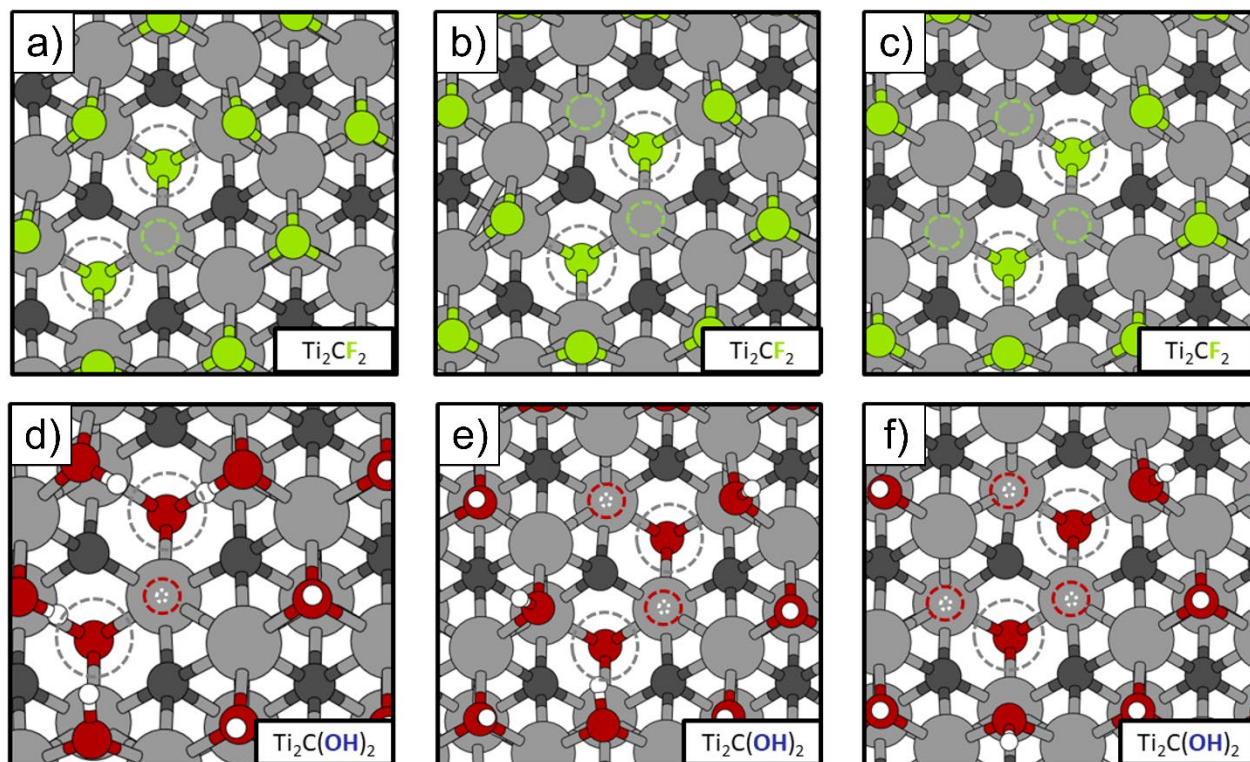


Figure S13. Relaxed substrates with $2V_{\text{Ti}} + qV_{\text{T}}$ (with $m=1,2,3$) clusters of vacancies for (a-c) Ti_2CF_2 and (d-f) $\text{Ti}_2\text{C}(\text{OH})_2$. (a and d) $2V_{\text{Ti}} + 1V_{\text{T}}$ cluster; (b and e) $2V_{\text{Ti}} + 2V_{\text{T}}$ cluster; (c and f) $2V_{\text{Ti}} + 3V_{\text{T}}$ cluster. Missing atoms are indicated with dashed circles. Surface reconstruction is similar to Figure S11. The lack of Ti atoms causes the surrounding terminations to move away from their lattice position, to increase the interaction with the remaining titanium atoms. The -OH groups (d-f) can rotate to stabilize the surface, pointing their hydrogen atom towards any accumulation of charge.